doi:10.1016/j.matchar.2009.12.008

Chemical analysis of a single basic cell of porous anodic aluminium oxide templates

François Le Coz, Laurent Arurault, Lucien Datas*

Université de Toulouse, CIRIMAT, UPS/INPT/CNRS, LCMIE, Bat 2R1, 118 Route de Narbonne, 31062 Toulouse Cedex 9, France

A B S T R A C T

We prepared anodic aluminium oxide (AAO) templates with "honeycomb" geometry, i.e. hexagonally ordered circular pores. The structures were extensively studied and characterized by EPMA coupled with FEG-SEM and FEG-TEM coupled with EDX at meso and nanoscopic scales, in other words, at the scale of a single basic cell making up the highly ordered porous anodic film. The analyses allowed the identification of the chemical compounds present and the evaluation of their levels in the different parts of each cell. Of note was the absence of phosphates inside the "skeleton" and their high content in the "internal part". Various models of porous anodic film growth are discussed on the basis of the results, contributing to a better understanding of AAO template preparation and self-nanostructuring phenomena.

Keywords:
AAO template
Mesoporosity
Chemical characterization
Anodization

1. Introduction

The porous anodization of aluminium and its alloys is a well-established process, widely used in various industrial fields such as aeronautics, architectural decoration or anti-corrosion protection. About twenty years ago, there was a renewal of interest in this process due to the pioneering research works of Masuda and Fukuda [1] and Gösele et al. [2], showing that under particular anodizing conditions it is possible to obtain highly ordered templates based on anodic aluminium oxide (AAO) and to then use the templates to prepare nano-devices, such as dots or wires [3–5].

Despite many academic and industrial studies, anodic film growth in general, and self-assembly of pores in particular, and the chemical composition of anodic films are still open to discussion because they depend on many operational parameters. For example, the chemical composition of anodic films directly depends on the nature of the aluminium alloy, the anodizing electrolyte, and the electrical conditions applied during the anodization.

The anodic films have also been reported [6–14] to be amorphous and, in fact, include a variable mixture of aluminium compounds: hydroxyl $Al(OH)_3$, oxy-hydroxyl AlOOH, or hydrated oxides Al_2O_3,xH_2O.

In 1979, Thibault and Duchemin [15] discovered that anodic films obtained in sulphuric and phosphoric baths include chemical elements originating from the electrolyte, such as sulphates or phosphates. Similarly in 1989 Farnan et al. [16] proved oxalate incorporation into the anodic films obtained using oxalic baths. During this period, chemical analyses considered the anodic films from a global point of view, i.e. at a scale higher than the micrometer.

Keller et al. [17] was the first to propose a general model of the anodic porous film, based on a set of unitary basic meso or nanocells, each including a pore. In 1986, Wada et al. [12] showed, using TEM cross-section views of a sulphuric anodic film, that the cell walls include five different layers. Moreover, Thompson [13] explained anion incorporation from different electrolytes to the anodic films and more recently proposed a "flow model" to describe the growth of the film. However, the

* *Corresponding author*. Tel.: +33 561 556 148; fax: +33 561 556 163.
E-mail address: arurault@chimie.ups-tlse.fr (L. Arurault).

chemical composition of the different parts of the unit cell remains to be established exactly.

The aim of our study then was to extensively characterize the anodic films not only at the mesoscopic scale but also at the nanoscopic level (<20 nm) of a single basic cell.

In the present study, we prepared thick ordered phosphoric anodic films allowing us to distinguish and to characterize the different parts of a unit cell making up the AAO template.

2. Experimental

The substrate was pure aluminium (99.99%). All chemical compounds used were analytical grade. Aqueous electrolyte solutions were obtained using deionised water.

2.1. *Process of Elaboration*

As described elsewhere [18] the aluminium substrate (sample diameter 14 mm) was prepared by sanding (firstly using grit paper followed by felts soaked in alumina up to 1 micron) and then by annealing under nitrogen atmosphere at 450 °C for 1 h. Additional electropolishing was carried out at 25 V for 1 min in a Jacquet mixed solution composed of perchloric/acetic acids (34/66 vol.%).

Anodization was carried out without delay at 185 V for 4 h. The electrolyte was made up of a vigorously mixed 8 wt.% aqueous phosphoric acid solution, while an aluminium plate (99.99 wt.%, diameter 30 mm) was used as cathode. The temperature was regulated at −1.5 °C by a cryostat (Huber CC2), while the voltage was applied by an Invensys Lambda generator (300 V–5 A). After formation of the porous anodic film, the aluminium substrate was chemically dissolved using an 18 wt.% hydrochloric acid solution including copper chloride CuCl (0.1 mol/L).

2.2. *Microscopic and Chemical Analyses*

Field-emission gun transmission electron microscopy (FEG-TEM—JEOL JEM 2100F) was used, in image or diffraction mode, to determine the morphology of the pores (Fig. 1), i.e. the pores density (ρ), the pore diameter (d_p), the thickness of the porous layer (e_p), the thickness of the barrier (or compact) layer (e_b) and the percentage of the void volume (τ). FEG-TEM was coupled with an energy dispersive X-ray (EDX-PGT) spectrometer enabling EDX chemical analysis and mapping.

Elemental chemical analyses were obtained with EPMA coupled with a field-emission gun scanning electron microscopy (FEG-SEM). The accelerating voltage was adjusted at 6 kV to decrease the analysis volume up to $2 \cdot 10^{-3}\ \mu m^3$ (analysis diameter≈150 nm) in order to turn down the influence of porosity. Six measurements were recorded for each sample.

3. Results and Discussion

3.1. *Macroscale Characterization*

FEG-TEM plan view (Fig. 2) of the as-prepared anodic films showed that the porosity is well formed and highly ordered, the structure being similar to Keller's ideal model.

The morphological characteristics of these AAO templates are typically as follows:

pores density (ρ) $6.72 \cdot 10^{12}/m^2$
pores diameter (d_p) 180 ± 30 nm
thickness of the porous layer (e_p) 76 ± 1 μm
thickness of the barrier (or compact) layer (e_b) 150 ± 10 nm
and percentage void volume (τ) 18%.

EPMA coupled with FEG-SEM was used to determine the elementary chemical contents:

O	61.5 ± 0.6 at.%
Al	35.8 ± 0.5 at.%
P	2.7 ± 0.1 at.%.

The standard deviations are low (respectively 1, 2 and 4% relative) in this case.

As shown by our own results and in agreement with previous findings [6–14,19], the anodic films are composed of aluminium hydroxide $Al(OH)_3$, oxy-hydroxide AlOOH and hydrated alumina Al_2O_3; overall, these amorphous compounds can be written as $Al_2O_3.xH_2O$ with $0 \leq x \leq 3$. Phosphorus would

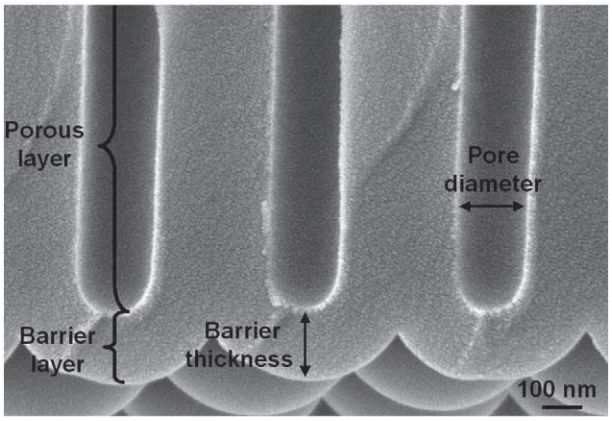

Fig. 1 – FEG-SEM cross-section view of a phosphoric anodic film.

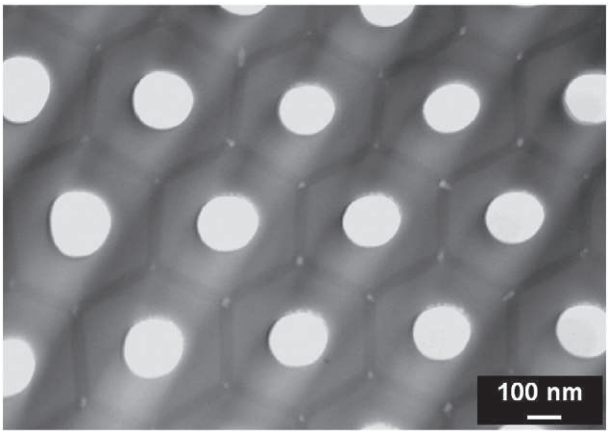

Fig. 2 – FEG-TEM plan view of a phosphoric anodic film.

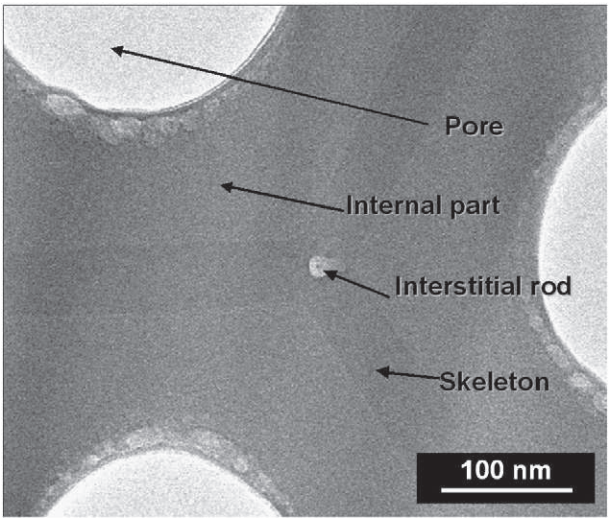

Fig. 3 – FEG-TEM plan view of a phosphoric anodic film, showing its different parts (the skeleton, the internal part and the interstitial rod).

form aluminium phosphates [9–11], especially monophosphate ($AlPO_4$) or trihydroxide phosphate of aluminium ($Al_2PO_4(OH)_3$); these two compounds can be written $2AlPO_4$, $y(Al_2O_3.3H_2O)$ with $y=0$ or 1.

Working on the hypothesis that the compounds are stoichiometric ($x=0$, 1 or 3) and the hydrogen is only involved in water molecules, the global chemical composition of the anodic film can be calculated from the P, Al and O contents obtained by EPMA coupled with FEG-SEM. The corresponding global atomic composition would then be:

$$Al_2O_3, 0.197AlPO_4, 0.034H_2O.$$

This result is in agreement with those of Thompson [13] and Mata-Zamora and Saniger [10], the anodic film always including significant levels of phosphorus.

3.2. *Characterization at Meso and Nanoscales*

Anodic films were observed at the nanoscopic scale using the FEG-TEM. The detailed structure of a unit basic cell (Fig. 3) includes different distinct parts:

- a hexagonal structure, called the "skeleton", which makes up the common internal walls between the unit cells,
- an "internal part", between the central pore and the skeleton,
- a point, called the "interstitial rod" inside the skeleton, at the intersection of three skeleton walls. Until now this interstitial rod had never been mentioned, perhaps due to its size. Its diameter is about 14 nm.

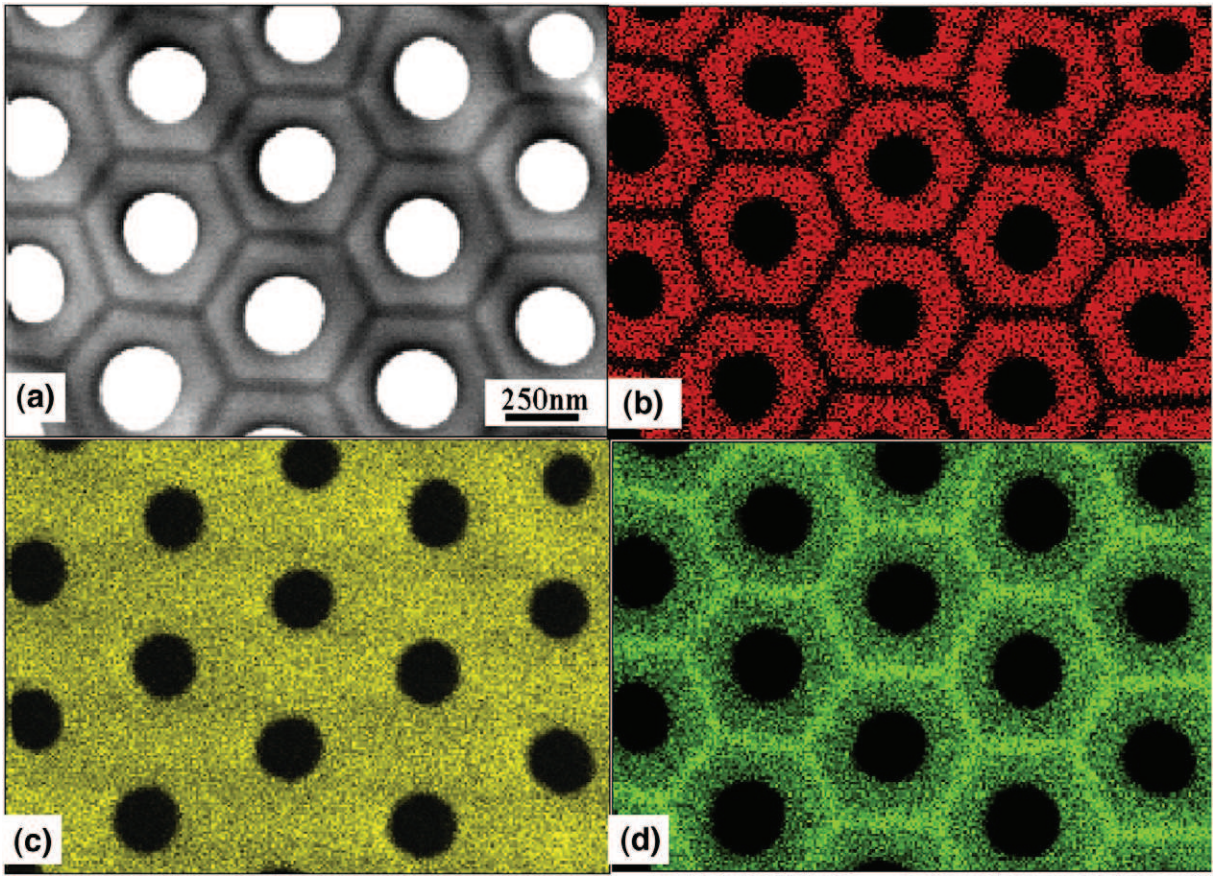

Fig. 4 – FEG-TEM plan view (a) of a phosphoric anodic film and corresponding X-ray maps of the elements (b) phosphorus, (c) oxygen and (d) aluminium.

The EDX chemical maps (Fig. 4), based on the Kα rays, especially of the elements aluminium and phosphorus, show the high chemical heterogeneity between the different parts of the unit cell, especially the skeleton and the internal part. The skeleton is mainly made up of aluminium and oxygen elements, while the internal part includes a high content of phosphorus elements. However, the oxygen map has to be carefully considered because there is the possibility of contamination during sample preparation under ambient atmosphere. The interstitial rod, however, was not distinguishable using this kind of chemical mapping.

Additional EDX analyses were performed on different points: on the skeleton (points 1 and 2), on the interstitial rod (point 3) and the internal part (points 4, 5 and 6) (Fig. 5).

The changes of the P/Al atomic ratio (Fig. 6), confirm that the internal part (points 4, 5, and 6) has a high phosphorus content. In contrast, the interstitial rod appears to have only a very low proportion of phosphorus (point 3), and the skeleton has none (points 1 and 2).

Fig. 7 shows that the Al/O atomic ratio is higher for the skeleton (points 1 and 2) and the interstitial rod (point 3) than for the internal part (points 4, 5, and 6). Moreover, the Al/O ratio increases inside the internal part from the skeleton to the pore wall.

All the EDX analyses primarily confirm the high heterogeneity of the elemental composition between the different parts of the unit cell, especially between the skeleton and the internal part. Furthermore, the lack of phosphorus in the skeleton is clearly shown. Considering solely the formation of the stoichiometric compounds Al_2O_3, $AlPO_4$ and H_2O, the composition of each part of the unitary cell can then be described as:

- Al_2O_3, $x_1.H_2O$ for the skeleton
- Al_2O_3, $0.018AlPO_4$, $x_2.H_2O$ for the interstitial rod
- Al_2O_3, $0.24AlPO_4$, $x_3.H_2O$ for the internal part.

3.3. *Crystallization of the Anodic Films on the Nanoscale*

During these FEG-TEM analyses, crystallization of the skeleton—and only the skeleton—was observed when the duration of exposure to the beam was sufficient (Fig. 8). The diffraction mode of the FEG-TEM was then used to highlight the crystallization of the different parts of the structure (Fig. 9).

The internal part and the skeleton were initially both amorphous. This amorphous state persisted in the case of the internal part after 30 s of beam exposure, while the skeleton became crystallized. Similar results [20] have been explained by differences in anion incorporation and in the amount of water. Here, the phosphorus compounds seem to stabilize the oxidized forms of aluminium included in the internal part at least during the first instants. Furthermore, this observation is in agreement with the previous TG–DTA results obtained by Mata-Zamora and Saniger using phosphoric, oxalic and sulphuric anodic usual films [10].

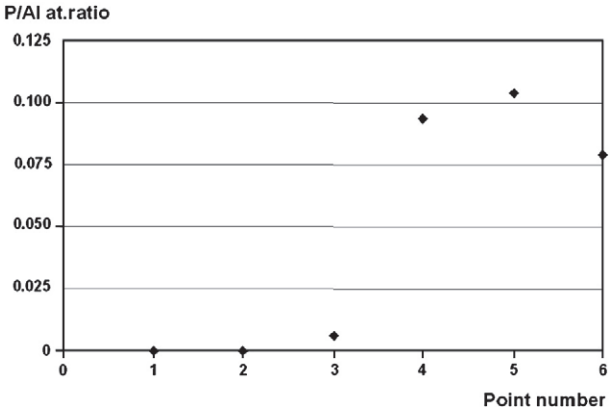

Fig. 6 – Phosphorus to aluminium atomic ratio.

3.4. *Growth Mechanisms of the AAO Templates*

The formation and growth of the anodic films are usually studied with either a transient or a permanent electrical regime. From the material point of view, the transients usually correspond to the appearance of pores [21–27], while permanent conditions refer to the steady-state growth of the anodic films. In 1953, Keller et al. [17] proposed a model describing an ideal microstructure of the anodic films obtained in the

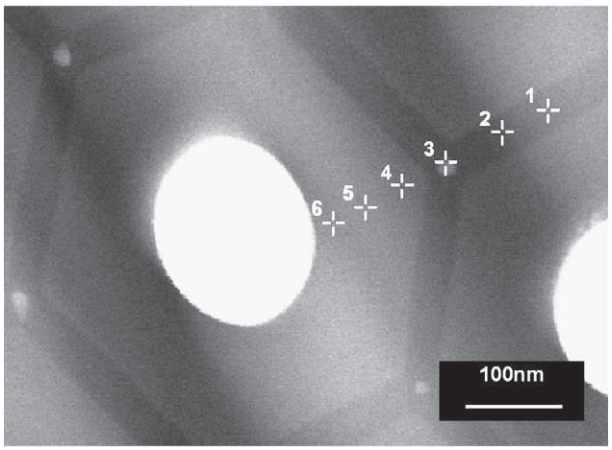

Fig. 5 – FEG-TEM plan view of a phosphoric anodic film showing the points analysed.

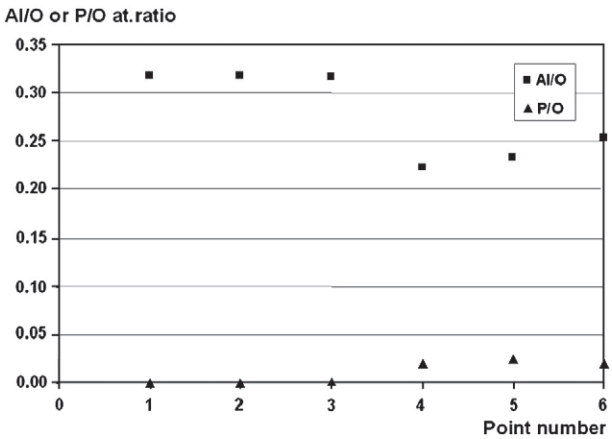

Fig. 7 – Atomic ratios of Al to O, and P to O at the different points.

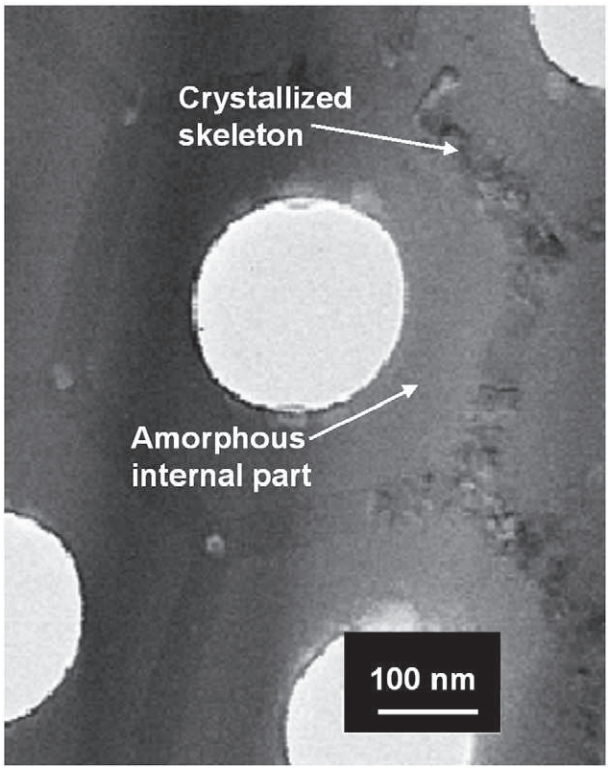

Fig. 8 – Crystallized skeleton after 30 s exposure to the electron beam of the FEG-TEM.

steady-state regime. Hexagonal cells, each surrounding a cylindrical pore, grow perpendicularly to the initial aluminium surface. Hoar and Yahalom [28] suggested that the growth mechanisms are based on the migration of O^{2-}, OH^- and Al^{3+} ions through the barrier layer. In 1978, Thompson et al. [29] completed this model, suggesting that aluminic ions Al^{3+} are initially ejected through the barrier layer and then precipitated with the anions from the anodizing bath, while Fukuda and Fukushima [30] considered anion transfer, especially of sulphates, through the compact layer.

From TEM cross-section views, Wada et al. [12] proposed, in 1986, an innovating model of the anodic film structures, including five different layers highlighted by TEM observations. Then, using xenon [13] and tungsten [31], Thompson showed that phosphate total incorporation was about 6–8 wt.% in the whole anodic film. These results were explained by anion adsorption on the surface of the barrier layer and by the incorporation of the most mobile species in this layer. Thus, the differences between PO_4^{3-} and O^{2-} mobilities could explain the incomplete incorporation of the phosphates.

Moreover, Thompson's team proposed a new growth model, called the flow model [31], based on the flow of material from the barrier layer to the "cell wall regions".

These different growth models are not totally contradictory but are partly complementary. However, they do not totally explain the observed structure, especially the interstitial rod.

Our results suggest that the absence of phosphates inside the skeleton and their high levels surrounding the pore seem to indicate that the skeleton has no contact with the anodizing electrolyte, while the internal part interacts with the bath. Moreover, EDX chemical mapping corroborated, for the phosphoric anodization, the flow model [31], i.e. a growth of the porous layer resulting partly from the ascent of the barrier layer; a phenomenon perhaps due to electrostriction and internal stress phenomena [32]. But, it is still difficult to explain the formation of the interstitial rod, located right in the heart of skeleton and including phosphorus from the electrolyte.

4. Conclusions

AAO templates were prepared by anodization in phosphoric electrolyte. These highly ordered films were then extensively characterized on different scales. In particular, the analyses showed that the as-prepared AAO film is in fact amorphous, partially hydrated and that its initial global chemical composition can be described, in agreement with previous works, as:

$$Al_2O_3, 0.197AlPO_4, 0.034H_2O.$$

The analyses (by EPMA coupled with FEG-SEM, TEM coupled with EDX) clearly indicated the heterogeneous chemical composition of the different parts of the unit cell. To sum up, the

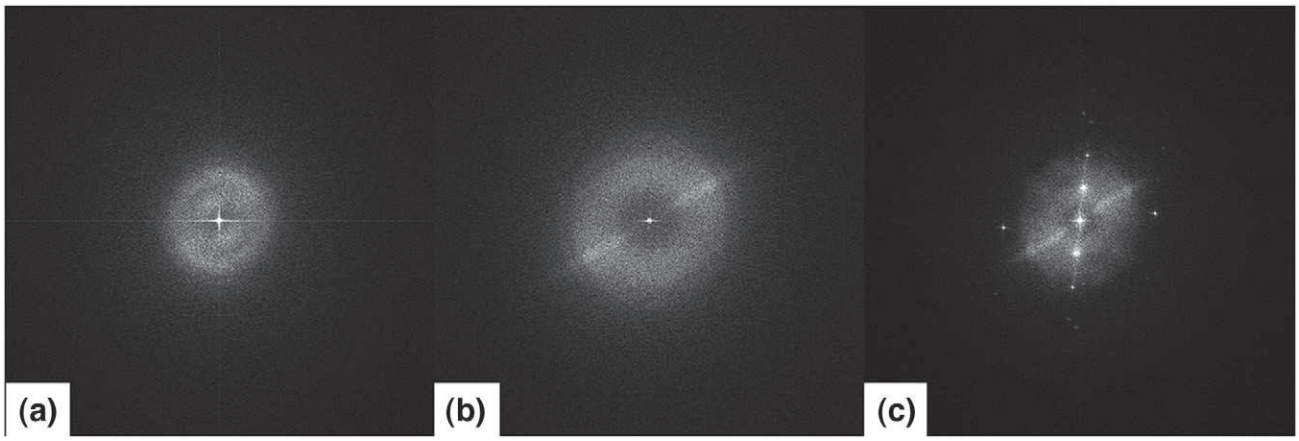

Fig. 9 – FEG-TEM observations, obtained in diffraction mode, of (a) the internal part, (b) the skeleton of the as-prepared anodic film, and (c) the skeleton after 30 s of exposure to the electron beam.

current study demonstrated the existence of different chemical compositions:

Al_2O_3, x_1H_2O for the skeleton
Al_2O_3, $0.018AlPO_4$, x_2H_2O for the interstitial rod
Al_2O_3, $0.24AlPO_4$, x_3H_2O for the internal part.

Furthermore, these permanent regime results confirmed the growth of the skeleton from the barrier layer in accordance with the "flow model". However, the presence of interstitial rods inside the skeleton was experimentally demonstrated for the first time. Knowing the chemical composition of the different parts of the basic cell is essential for understanding and improving any planned functionalization—for example by chemical grafting—of the AAO phosphoric templates.

Acknowledgements

The authors thank Peter Winterton for his helpful comments and Philippe De Perseval (LMTG) for the EPMA coupled with FEG-SEM facilities at the GeoForschungsZentrum (GFZ) in Potsdam (Germany).

REFERENCES

[1] Masuda H, Fukuda K. Ordered metal nanohole arrays made by a two-step replication of honeycomb structures of anodic alumina. Science 1995;268:1466–8.
[2] Jessensky O, Müller F, Gösele U. Self-organized formation of hexagonal pore arrays in anodic alumina. Appl Phys Lett 1998;72(10):1173–5.
[3] Inoue S, Chu S-L, Wada K, Li D, Maneda H. New roots to formation of nanostructures on glass surface through anodic oxidation of sputtered aluminium. Sci Technol Adv Mater 2003;4:269–76.
[4] Wang J, Ma Y, Watanabe K. Magnetic-field-induced synthesis of magnetic γ-Fe_2O_3 nanotubes. Chem Mater 2008;20:20–2.
[5] Wang Y, Gösele U, Steinhart M. Mesoporous polymer nanofibers by infiltration of block copolymers with sacrificial domains into porous alumina. Chem Mater 2008;20:379–81.
[6] Sharma AK, Bhojaraj H. Thermoanalytical studies of anodic oxide coatings on aluminium. Plating Surf Finish 1989:59–61.
[7] Mardilovich PP, Govyadinov AN, Mukhurov NI, Rzhevskii AM, Paterson RJ. New and modified anodic alumina membranes; part. I. Thermotreatment of anodic alumina membranes. Membr Sci 1995;98:131–42.
[8] Burgos N, Paulis M, Montes M. Preparation of Al_2O_3/Al monoliths by anodisation of aluminium as structured catalytic supports. J Mater Chem 2003;13:1458–67.
[9] Bocchetta P, Sunseri C, Chiavarotti G, Di Quarto F. Microporous alumina membranes electrochemically grown. Electrochim Acta 2003;48:3175–83.
[10] Mata-Zamora ME, Saniger JM. Thermal evolution of porous anodic aluminas: a comparative study. Rev Mex Fis 2005;51(5):502–9.
[11] Kirchner A, MacKenzie KJD, Brown IWM, Kemmitt T, Bowden ME. Structural characterisation of heat-treated anodic alumina membranes prepared using a simplified fabrication process. J Membr Sci 2007;287:264–70.
[12] Wada K, Shimohira T, Yamada M, Baba N. Microstructure of porous anodic oxide films on aluminium. J Mater Sci 1986;21:3810–6.
[13] Thompson GE. Porous anodic alumina: fabrication, characterization and applications. Thin Solid Films 1997;297:192–201.
[14] Melendres CA, Van Gils S, Terryn H. Toward a quantitative description of the anodic oxide films on aluminium. Electrochem Commun 2001;3:737–41.
[15] Thibault S, Duchemin C. Optical reflectance method for analyzing anodic films formed on aluminium. Corros NACE 1979;35(11):532–3.
[16] Farnan I, Dupree R, Jeong Y, Thompson GE, Wood GC, Forty AJ. Structural chemistry of anodic alumina. Thin Solid Films 1989;173:209–15.
[17] Keller F, Huntey MS, Robinson DL. Structural features of oxide coatings on aluminium. J Electrochem Soc 1953;100:411–9.
[18] Le Coz F. PhD thesis, Paul Sabatier University, Toulouse III, France 2007.
[19] Zamora G. PhD thesis, Paul Sabatier University, Toulouse III, France 2004.
[20] Lopez V, Otero E, Escudero E, Gonzalez JA. Nanostructural changes in porous anodic films on aluminum during aging. Surf Coat Technol 2002;154:34–41.
[21] Goad DGW, Dignam MJ. Transient response of the system Al/Al_2O_3/electrolyte. Part I. Galvanostatic transients. Can J Chem 1972;50(20):3259–66.
[22] Patermarakis G, Lenas P, Karavassilis C, Papayiannis G. Kinetics of growth of porous anodic Al_2O_3 films on Al metal. Electrochim Acta 1991;3:709–25.
[23] Parkhutik VP, Shershulsky VI. Theoretical modelling of porous oxide growth on aluminium. J Phys D Appl Phys 1992;25:1258–63.
[24] Wu H, Herbert KR. Electrochemical transients during the initial moments of anodic oxidation of aluminium. Electrochim Acta 2002;47:1373–83.
[25] Wu H, Herbert KR. Reply to comments on electrochemical transients during the initial moments of anodic oxidation of aluminium. Electrochim Acta 2002;48(2):131–3.
[26] Le Coz F, Arurault L, Bes RS. Study of the initial electrical transient during the growth of the anodic porous layers. ATB Metallurgie 2006;45(1–4):489–92.
[27] Le Coz F, Arurault L, Bes RS. Simulation of the electrical transient during the porous anodizing of pure aluminium substrate. In: DeGiorgi VG, Brebbia CA, Adey RA, editors. Simulation of electrochemical processes II. Southampton: WIT Press; 2007. p. 163–72.
[28] Hoar TP, Yahalom J. The initiation of pores in anodic oxide films formed on aluminium in acid solution. J Electrochem Soc 1963;100(6):614–21.
[29] Thompson GE, Furneaux RC, Wood GC, Richardson JA, Goode JS. Nucleation and growth of porous anodic films on aluminium. Nature 1978;272:433–5.
[30] Fukuda Y, Fukushima T. Behavior of sulfate ions during formation of anodic oxide film on aluminium. Bull Chem Soc Jpn 1980;53:3125–30.
[31] Garcia-Vergara SJ, Skeldon P, Thompson GE, Habazaki H. A flow model of porous anodic film growth on aluminium. Electrochim Acta 2006;52:681–7.
[32] Zakeri R, Watts C, Wang H, Kohli P. Synthesis and characterization of nonlinear nanopores in alumina films. Chem Mater 2007;19:1954–63.